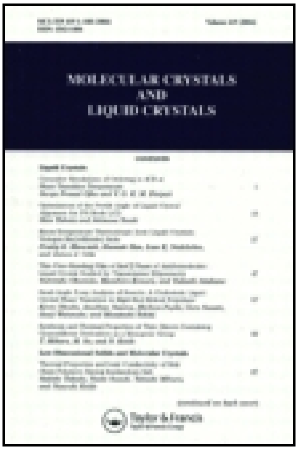

Molecular Crystals and Liquid Crystals Incorporating Nonlinear Optics
Publication details, including instructions for authors and subscription information:
http://www.tandfonline.com/loi/gmcl17

Calorimetric Study of Nonyloxybenzoyloxy-cyanoazobenzene (9OBCAB)

P. Leach [a], P. Das [a], C. W. Garland [a] & R. Shashidhar [b]

[a] Department of Chemistry and Center for Materials Science and Engineering, Massachusetts Institute of Technology, Cambridge, MA, 02139

[b] Raman Research Institute, Bangalore, 560 080, India

Version of record first published: 04 Oct 2006.

To cite this article: P. Leach, P. Das, C. W. Garland & R. Shashidhar (1989): Calorimetric Study of Nonyloxybenzoyloxy-cyanoazobenzene (9OBCAB), Molecular Crystals and Liquid Crystals Incorporating Nonlinear Optics, 168:1, 183-188

To link to this article: http://dx.doi.org/10.1080/00268948908045970

Mol. Cryst. Liq. Cryst., 1989, Vol. 168, pp. 183–188
Reprints available directly from the publisher
Photocopying permitted by license only

Printed in the United States of America

Calorimetric Study of Nonyloxybenzoyloxy-cyanoazobenzene (9OBCAB)

P. LEACH, P. DAS and C. W. GARLAND
Department of Chemistry and Center for Materials Science and Engineering, Massachusetts Institute of Technology, Cambridge, MA 02139

and

R. SHASHIDHAR
Raman Research Institute, Bangalore 560 080, India

(Received August 1, 1988; in final form September 1, 1988)

Calorimetric studies of 9OBCAB have been made using DSC and high-resolution ac techniques. A small heat capacity peak associated with the smectic-A_d(SmA_d)-reentrant nematic (N_r) second-order transition has been observed. Analysis in terms of the critical exponent α suggests the possibility of Fisher renormalization at this SmA_d–N_r transition. DSC measurements have shown the presence of two metastable crystal phases (denoted CrX and CrY) as well as the equilibrium CrK crystal phase. The latent heats for first-order transitions among these crystal phases and for the N_r–CrX and N_r–CrK melting/freezing transitions have been determined. The transition from N_r into the monotropic monolayer smectic-A phase was preempted in our experiments by $N_r \rightarrow$ CrX freezing.

Reentrant smectic polymorphism in pure compounds was first observed in 4-*n*-octyloxybenzoyloxy-4′-cyanostilbene (T8),[1] which exhibits the phase sequence $N \rightarrow SmA_d \rightarrow N_r \rightarrow SmA_1$ where SmA_d is a partial bilayer smectic-A phase, SmA_1 is a monolayer smectic-A phase, and N and N_r are both nematic phases. These transitions in T8 have been studied with x-ray techniques,[2,3] calorimetry,[3,4] and frustrated spin-gas theory,[5] with emphasis on the SmA_d–N_r and N_r–SmA_1 critical behavior. Unfortunately, the transition temperatures in T8 decrease as a function of time and the excess heat capacity ΔC_p peaks are quite small. This limits the quality of theoretical fits to ΔC_p, especially $\Delta C_p(A_dN_r)$ which is only 30 percent of $\Delta C_p(N_rA_1)$.

The compound 4-nonyloxybenzoyloxy-4′-cyanoazobenzene (9OBCAB)

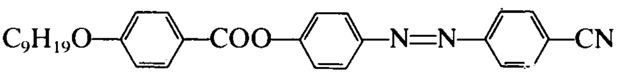

is isostructural and isoelectronic with T9. However, nOBCAB molecules have a —N=N— azo linking group in place of the —CH=CH— group in Tn molecules; thus the former are much more stable at high temperatures. It has been reported previously[6] that 90BCAB exhibits the same reentrant polymorphism as T8. On cooling, the phase sequence is

$$\mathrm{I} \xrightarrow[516.1\mathrm{K}]{} \mathrm{N} \xrightarrow[485.6\mathrm{K}]{} \mathrm{SmA}_d \xrightarrow[389.2\mathrm{K}]{} \mathrm{N}_r \xrightarrow[344.1\mathrm{K}]{} \mathrm{SmA}_1$$

Note that the SmA_1 phase is monotropic since the equilibrium CrK phase melts at 367K to yield N_r.

An ac calorimetric technique[7] has been used to study the lower temperature transitions in 90BCAB. As expected, a second-order SmA_d–Nr heat capacity peak was observed that was small but still ~2.5 times larger than that in T8. On the basis of theoretical modelling,[5] one would expect that the N_r–SmA_1 heat capacity peak would also be substantially larger than that in T8 and thus ideal for critical analysis. Unfortunately and contrary to expectations based on x-ray and microscopic studies,[6] we have not been able to observe a N_r–SmA_1 transition in 90BCAB. On cooling our sample, the N_r phase froze into a metastable crystal form at 349.1K even using a fast (for ac calorimetry) scan rate of -1.5 K h^{-1}. This freezing transition was strongly first order with no evidence of pretransitional fluctuation effects. The C_p values decreased discontinuously by 0.26 J K^{-1} g^{-1} on going from the N_r phase to the crystalline phase.

The excess specific heat capacity associated with the SmA_d–N_r transition is defined by

$$\Delta C_p(\mathrm{A}_d\mathrm{N}_r) = C_p(\mathrm{obs}) - C_p(\mathrm{background}) \tag{1}$$

where C_p(obs) is the observed specific heat capacity near T_c and C_p(background) $= 2.55 - 0.004(T - 380)$ J K^{-1} g^{-1}, which describes the linear noncritical C_p variation observed over the 350–380K range. The resulting ΔC_p variation is shown in Figure 1. Note that this is quite a small peak: $\Delta C_p(\mathrm{max}) \simeq 0.10$ J K^{-1} g^{-1} at T_c. The integrated enthalpy $\delta H \equiv \int \Delta C_p\, dT$ for this SmA_d–N_r peak is only 0.20 J g^{-1}, which is larger than the SmA_d–N_r value of 0.08 J g^{-1} for T8[5] but small compared to more typical N–SmA_d values which range from 0.33 J g^{-1} (80CB) to 0.75 J g^{-1} (8CB).[8] Fortunately, no drift in T_c was observed over a period of ~100 h. Thus a slow scan rate of 45 mK h^{-1} could be used over the range $|T - T_c| <$ 0.43K. For this inner range, the points shown in Figure 1 are a merged set obtained by averaging pairs of adjacent data points. In systems exhibiting weak first-order transitions and two-phase coexistence, anomalous phase shifts occur in the ΔT_{ac} signal.[7] No such anomalous phase shifts were observed near T_c for 90BCAB, and the SmA_d–N_r transition is second order as expected.[3,5]

An attempt has been made to fit the excess heat capacity data in Figure 1 with the critical fluctuation form

$$\Delta C_p^{\pm} = A^{\pm}|t|^{-\alpha}(1 + D^{\pm}|t|^{0.5}) + B \tag{2}$$

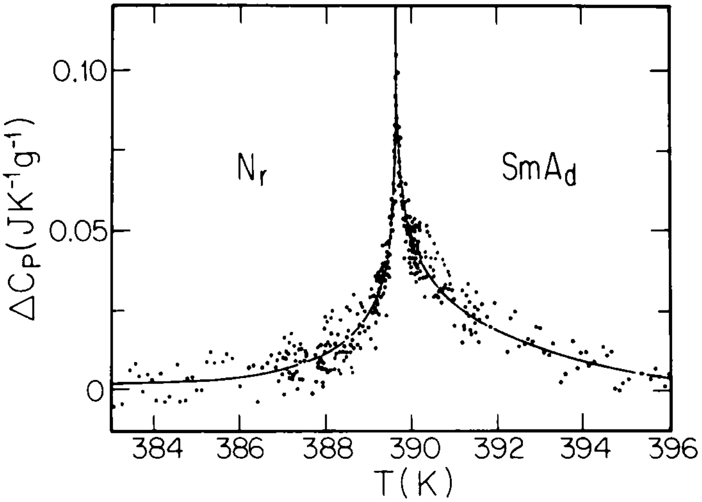

FIGURE 1 Excess heat capacity ΔC_p associated with the SmA_d–N_r phase transition in 90BCAB. This peak is very small; the maximum ΔC_p value is only 4 percent of the C_p(background) value at T_c. The smooth curve represents Equation (2) using the parameters of fit 4 in Table I.

where $t \equiv (T - T_c)/T_c$. Two fitting ranges were used. Range I contains 270 data points with $|T - T_c| < 0.43$K or $|t| < 1.1 \times 10^{-3}$, and the corrections-to-scaling coefficients $D^{\pm}$ are set equal to zero. Range II contains 463 points with $|T - T_c| < 6.4$K or $|t| < 1.6 \times 10^{-2}$. The parameters obtained from least-squares fitting are given in Table I. The best fit gave $\alpha \simeq -0.1$, and the parameters were stable on range shrinking; see fits 3 and 4. Unfortunately, the χ_ν^2 minimum is very broad, and a wide range of α values ($+0.05$ to -0.2) are consistent with these data. This is, however, the first set of $\Delta C_p(A_dN_r)$ data for which an analysis can even be attempted. In other systems studied with high-resolution calorimetric techniques, either $\Delta C_p(A_dN_r)$ was much too small[5] or the SmA_d–N_r transition was monotropic and the sample froze at a temperature above T_c.[9]

The fact that the data are consistent with a negative critical exponent α as large as -0.2 suggests the possibility of Fisher renormalization.[10] Although the present

TABLE I

Values of the adjustable parameters obtained from least-squares fits of $\Delta C_p(A_dN_r)$ using Eq. (2). Values in parentheses were held fixed during the fit. The units are K for T_c and J K^{-1} g^{-1} for A and B; the standard deviation σ was taken to be 0.006, which is 0.23% of C_p(obs). Range I is $|t| < 1.1 \times 10^{-3}$ and range II is $|t| < 1.6 \times 10^{-2}$.

Fit	Range	T_c	α	A^+	A^-/A^+	D^+	D^-/D^+	B	χ_ν^2
1	I	389.608	(0.05)	0.1985	0.947	(0)	(1)	−0.235	1.38
2	II	389.610	(0.05)	0.2105	0.943	0.110	2.10	−0.252	1.44
3	I	389.611	−0.106	−0.3268	1.093	(0)	(1)	0.201	1.30
4	II	389.610	−0.109	−0.3289	1.136	−0.570	2.42	0.198	1.36
5	I	389.611	(−0.2)	−0.3168	1.203	(0)	(1)	0.126	1.41
6	II	389.610	(−0.2)	−0.3512	1.245	−1.327	1.98	0.132	1.38

$\Delta C_p(A_dN_r)$ data cannot resolve this point, x-ray results[3] on the analogous SmA$_d$–N$_r$ transition in T8 support the idea of Fisher renormalization. As shown in Table II, the critical exponents γ, $\nu_{\parallel}$, and $\nu_{\perp}$ for the susceptibility and the correlation lengths in T8 correspond rather well with Fisher renormalized versions of known N–SmA$_d$ exponents. The criterion for the presence of Fisher renormalization is a large magnitude for $(dT_c/dX)^2$, where X is the mole fraction of the species in a binary mixture. Fisher renormalization does not occur in 8CB + 10CB mixtures (dT_c/dX = 10.8K), but it does occur in DB$_6$ + TBBA (dT_c/dX = 150 K) and $\bar{7}$S5 + 80CB (dT_c/dX = 289 K).[13,14] The value of dT_c/dX for T7 and T8 mixtures close in composition to pure T8 is 108K,[4] which is large enough to make Fisher renormalization likely. The value of dT_c/dX for 80BCAB + 90BCAB mixtures close in composition to pure 90BCAB is 39 K.[15] This yields an intermediate value for $(dT_c/dX)^2$, 13 times larger than that for 8CB + 10CB but 13 times smaller than that for T8, making it likely that partial rather than complete Fisher renormalization occurs in 90BCAB.

An extensive series of differential scanning calorimetry (DSC) runs were carried out in order to characterize the metastable freezing/melting transitions in 90BCAB. Both heating and cooling runs were made, mostly at a scan rate of 10 K min^{-1} although the effect of other scan rates was explored. Several sharp first-order transitions were observed, revealing the presence of two metastable crystalline phases (CrX and CrY) as well as the equilibrium CrK phase that is originally present at room temperature in a fresh sample. Most of the DSC results are summarized in Figure 2. The slopes of the H(T) enthalpy curves for different single phases are based on our ac heat capacity values for the N$_r$ and CrX phases and the assumption that C_p for CrK is approximately the same as that for CrX over the small range from 335K to 367K.

The only transition observed with DSC on heating a fresh sample from room temperature is the CrK → N$_r$ melting since the N$_r$ → SmA$_d$ transition enthalpy is too small to be observed. The CrK–N$_r$ latent heat is 82 ± 3 J g^{-1}.[16] On cooling at 10 K min^{-1}, N$_r$ freezes to CrX at 335 ± 2K with an enthalpy change of 46 ± 5 J g^{-1}. For faster scans, this transition lies lower in temperature (331K at 25 K

TABLE 2

Critical exponents for various N-SmA$_d$ transitions. Fisher renormalization yields exponents $\alpha_R = -\alpha/(1-\alpha)$, $\gamma_R = \gamma/(1-\alpha)$, $\nu_R = \nu/(1-\alpha)$.

Material	γ	$\nu_{\parallel}$	$\nu_{\perp}$	α
XY model[a]	1.32	0.67	0.67	−0.01
CBOOA[b]	1.30	0.70	0.62	0.15
80CB[c]	1.32	0.71	0.58	0.2
FishRN-CBOOA	1.53	0.82	0.73	−0.18
FishRN-80CB	1.65	0.89	0.73	−0.25
T8[d]	1.53	0.88	0.76	—

[a] Ref. 11
[b] Ref. 12
[c] Ref. 8
[d] Ref. 3

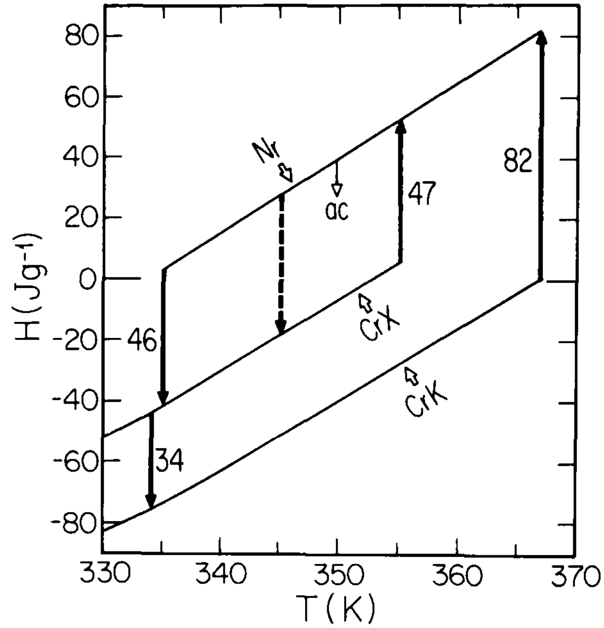

FIGURE 2 Enthalpy-temperature diagram for 90BCAB. The slopes of the H(*T*) lines in various phases are based on ac heat capacity values (see text). The latent heat values (in Jg^{-1}) given on the vertical transition lines are obtained from DSC measurements. The dashed arrow between the N_r and CrX lines indicates that this transition occurred isothermally after cooling the N_r phase rapidly to 345K and then holding the temperature constant. The arrow labelled *ac* marks the temperature where N_r froze on an ac calorimeter scan at −0.025K/min.

min^{-1} and 325K at 40 K min^{-1}). Note also that the slow (0.025 K min^{-1}) ac calorimeter scans show $N_r \rightarrow$ CrX at 349K. If one cools at 10 K min^{-1} to 345K and then holds the temperature constant, the $N_r \rightarrow$ CrX transition occurs isothermally after 10 min with an enthalpy change of ~44 J g^{-1}. When the sample is then immediately heated up again, the CrX phase melts to N_r at 355K with a ΔH value of 47 J g^{-1}. This behavior and subsequent details described below make it clear that CrX is a new metastable crystals phase differing appreciably from CrK.

On cooling the CrX phase after it has formed at 335K, a small and reversible first-order transition to CrY is observed at ~307K (not shown in Figure 2). For scan rates of 10 K min^{-1}, the CrX → CrY change occurs at 305K on cooling and the CrY → CrX change occurs at 309K on reheating. In both cases, the enthalpy change is 8 ± 3 J g^{-1}.

If the CrX phase is heated after this CrX → CrY → CrX cycle has taken place, an endothermic transition from CrX to CrK occurs at ~334K. In one case, total conversion of CrX to CrK occurred with an enthalpy change of 34 J g^{-1}. Subsequent heating showed only the CrK → N_r melting peak. In three other cases, only partial conversion of CrX occurred. In these cases where equilibrium is not achieved, both a moderate size CrX → N_r peak at 355K and a smaller than usual CrK → N_r peak are observed. The CrX → CrK endotherm peak is either absent or very small and broad if the CrX phase is not cooled below 313 K. In one case, the CrX phase was held at 345 K for 20 min and no conversion to CrK was observed.

In summary, the excess heat capacity associated with the second-order SmA_d–N_r transition has been measured and analyzed for 90BCAB. The small $\Delta C_p(\mathrm{A}_d\mathrm{N}_r)$ peak is best described by a negative critical exponent α, which suggests that Fisher renormalization may occur. This could be best tested by an x-ray study like that made on T8.[3] The monotropic SmA_1 phase was not observed in our ac calorimetric measurements or in the DSC scans. In both cases, the N_r phase froze into metastable crystal forms that have been characterized by DSC measurements.

Acknowledgment

This work was supported in part by the National Science Foundation under grants DMR-8315637 and DMR-8702052.

References

1. A. M. Levelut, F. Hardouin and G. Sigaud, in *Liquid Crystals*, Proc. Int. Liquid Crystals Conf., Bangalore, 1979, S. Chandrasekhar, ed. (Heyden, London, 1980), p. 143.
2. F. Hardouin and A. M. Levelut, *J. Phys. (Paris)*, **41**, 41 (1980).
3. K. W. Evans-Lutterodt, J. W. Chung, B. M. Ocko, R. J. Birgeneau, C. Chiang, C. W. Garland, E. Chin, J. Goodby and Nguyen Huu Tinh, *Phys. Rev.*, **A36**, 1387 (1987).
4. C. Chiang and C. W. Garland, *Mol. Cryst. Liq. Cryst.*, **122**, 25 (1985).
5. J. O. Indekeu, A. N. Berker, C. Chiang and C. W. Garland, *Phys. Rev.*, **A35**, 1371 (1987) and references cited therein.
6. K. A. Suresh, R. Shashidhar, G. Heppke and R. Hopf, *Mol. Cryst. Liq. Cryst.*, **99**, 249 (1983).
7. C. W. Garland, *Thermochim. Acta*, **88**, 127 (1985).
8. G. B. Kasting, K. J. Lushington and C. W. Garland, *Phys. Rev.*, **B22**, 321 (1980); J. Thoen, H. Marynissen and W. Van Dael, *Phys. Rev.*, **A26**, 2886 (1982).
9. K. J. Lushington, G. B. Kasting and C. W. Garland, *Phys. Rev.*, **B22**, 2569 (1980).
10. M. E. Fisher, *Phys. Rev.*, **176**, 257 (1968); M. E. Fisher and P. E. Scesney, *Phys. Rev.*, **A2**, 825 (1970).
11. J. C. LeGuillon and J. Zinn-Justin, *Phys. Rev.*, **B21**, 3976 (1980).
12. J. Als-Nielsen, R. J. Birgeneau, M. Kaplan, J. D. Litster and C. R. Safinya, *Phys. Rev. Lett.*, **39**, 352 (1977); **41**, 1262(E) (1978).
13. M. E. Huster, K. J. Stine and C. W. Garland, *Phys. Rev.*, **A36**, 2364 (1987) and references cited therein.
14. C. W. Garland, C. Chiang and F. Hardouin, *Liq. Cryst.*, **1**, 81 (1986).
15. B. R. Ratna and R. Shashidhar, unpublished.
16. All CrK → N_r DSC curves showed two adjacent peaks: a small peak at 362.6 ± 0.4 K ($\sim$10 J g^{-1}) and a large peak at 366.9 ± 0.4K ($\sim$72 J g^{-1}). The total CrK–N_r latent heat was quite reproducible (82 ± 3 J g^{-1} on eight runs) but the relative size of the two peaks varied somewhat.